EPTT 2024
Escola de Primavera de Transição e Turbulência

ABCM
Associação Brasileira de Engenharia e Ciências Mecânicas

EPTT-2024-0025
LINEAR STABILITY ANALYSIS OF VISCOELASTIC BOUNDARY LAYER FLOWS

Beatriz Liara Carreira
Leandro Franco de Souza
Universidade de São Paulo, Instituto de Ciências Matemáticas e de Computação, São Carlos, SP
liara.carreira@usp.br, lefraso@icmc.usp.br

Abstract. *Understanding the flow regime, whether laminar or turbulent, is crucial in several scientific and industrial applications, especially in the laminar-turbulent transition process. This phenomenon, often triggered by sources of physical instabilities in the flow, can be observed in the boundary layer, where small amplitude disturbances, such as Tollmien-Schlichting waves, gradually amplify, resulting in the transition to turbulence. Given the importance of the effect of viscosity on the boundary layer and considering that this is also an important property of viscoelastic fluids, investigating and understanding the transition phenomenon in these flows is relevant and essential for several industrial applications. Therefore, the objective of this work is to investigate the hydrodynamic stability in a two-dimensional and isothermal boundary layer flow, considering an incompressible and non-Newtonian fluid represented by the Giesekus viscoelastic model, through the analysis of Tollmien-Schlichting wave convection using the Linear Stability Theory.*

Keywords: *laminar-turbulent transition, linear stability theory, viscoelastic fluid, boundary layer*

1. INTRODUCTION

In several scientific and industrial applications, understanding the flow regime, whether laminar or turbulent, is extremely relevant, especially when it comes to the transition from the laminar regime to the turbulent state. This process, known as laminar-turbulent transition, is generally triggered by physical sources of instabilities present in the flow, such as structural vibration, noise, surface roughness, or external turbulence.

In the boundary layer, the laminar-turbulent transition can be triggered by the growth of small-amplitude disturbances, such as Tollmien-Schlichting waves (Xu *et al.*, 2016). These waves are slowly amplified until they can eventually grow large enough that nonlinearities take control and the flow transitions to turbulence. Since the existence of Tollmien-Schlichting instability waves was confirmed by Schubauer and Skramstad (1948), many studies have been carried out to further explore and explain the transition.

The Linear Stability Theory is an already established technique, which consists precisely of obtaining the response of the flow to disturbances, with due interest in infinitesimal disturbances (Gennaro, 2012). It is therefore a suitable tool to investigate how the evolution of these disturbances is related to the (Zhang *et al.*, 2013) transition phenomenon.

On the other hand, many rheologically complex fluids, such as polymer solutions, soups, blood, shampoo, and ketchup cannot be described by the constitutive equation of the Newtonian model. These fluids exhibit a variety of non-Newtonian behaviors that cannot be captured using the Navier-Stokes equations (Cracco, 2019). It is for this reason that it is necessary to add a constitutive equation that represents the behavior of the non-Newtonian extra-stress tensor.

Even though the boundary layer theory has many applications, such as calculating the frictional drag of bodies in (Schilichting, 1979) flow, there are still many questions to be investigated. For example, there are studies on the investigation of the transition process from the boundary layer to Newtonian fluid (Souza *et al.*, 2002) and also on the transition of viscoelastic flows in other geometries, such as flow between parallel plates (Brandi *et al.*, 2019). However, especially with regard to the instability of viscoelastic fluids in the boundary layer, there is still much to explore.

In particular, non-Newtonian laminar boundary layer flows are observed in several domains, including biological and chemical systems, food processing engineering systems, or pharmaceutical processing (Amoo and Fagbenle, 2020). Since most of the differences between categories of non-Newtonian fluids are related to their viscosity, a dominant physical property within the boundary layer region, a thorough understanding of these flows is of considerable importance for various industrial applications (Amoo and Fagbenle, 2020).

Therefore, this work uses the Linear Stability Theory to investigate the convection of Tollmien-Schlichting waves in a

boundary layer flow over a flat plate, considering a viscoelastic fluid represented by the Giesekus model. The investigations were conducted by observing the behavior of the maximum spatial growth rates and the unstable regions delimited by the stability diagrams. Several cases were considered, obtained from the variation of dimensionless parameters characteristic of non-Newtonian flow. In this way, it was possible to analyze how the elastic forces and the polymeric contribution of the fluid influence the spatial stability of the viscoelastic flow, comparing them with Newtonian fluid flows.

2. MATHEMATICAL FORMULATION

Considering that the flow is two-dimensional and unsteady, then the continuity and momentum equations that govern the flow for an incompressible and non-Newtonian fluid, in its dimensionless form, are given by

$$\nabla \cdot \mathbf{u} = 0, \tag{1}$$

$$\frac{\partial \mathbf{u}}{\partial t} + \nabla \cdot (\mathbf{uu}) = -\nabla p + \frac{\beta_{nn}}{Re_L}\nabla^2 \mathbf{u} + \nabla \cdot \mathbf{T}, \tag{2}$$

where $\mathbf{u}$ denotes the velocity field, t is the time, p is the pressure and $\mathbf{T}$ is the non-Newtonian extra-stress tensor (symmetric), given by $\mathbf{T} = \begin{bmatrix} T^{xx} & T^{xy} \\ T^{xy} & T^{yy} \end{bmatrix}$.

The dimensionless parameter $Re_L = U_\infty L/\nu$ is associated with the Reynolds number, where L and U_∞ denote length and velocity scales, respectively, and ν is the kinematic viscosity of the fluid. The amount of Newtonian solvent is controlled by the dimensionless solvent viscosity coefficient $\beta_{nn} = \eta_s/\eta_0$, where $\eta_0 = \eta_s + \eta_p$ denotes the total shear viscosity, being η_s and η_p the Newtonian solvent and polymeric viscosities, respectively.

In this paper, we worked with viscoelastic fluid flow governed by the non-linear Giesekus constitutive equation (Giesekus, 1982), which is given by

$$\mathbf{T} + Wi\overset{\triangledown}{\mathbf{T}} + \alpha_G \frac{WiRe_L}{1-\beta_{nn}}(\mathbf{T}\cdot\mathbf{T}) = \frac{1-\beta_{nn}}{Re_L}(\nabla\mathbf{u} + \nabla\mathbf{u}^\top), \tag{3}$$

where α_G is the mobility parameter that regulates the shear thinning behavior of the fluid ($0 \leq \alpha_G \leq 1$), $\mathbf{T}\cdot\mathbf{T}$ is a tensor product and $\overset{\triangledown}{\mathbf{T}}$ is the upper-convected derivative. The dimensionless parameter $Wi = \lambda U_\infty/L$ is called Weissenberg number, being λ the relaxation-time of the fluid.

3. LINEAR STABILITY THEORY

Through the Linear Stability Theory (LST), it is possible to obtain answers regarding the growth or decay of infinitesimal disturbances imposed on the base flow. Therefore, the instantaneous flow components can be decomposed into base flow, considered two-dimensional and non-parallel in this work, plus a disturbed part

$$\mathbf{q}(x,y,t) = \hat{\mathbf{q}}(x,y) + \tilde{\mathbf{q}}(x,y,t), \tag{4}$$

where $\hat{\mathbf{q}}(x,y) = (U,V,P,\hat{\mathbf{T}})$ describes the components of the base flow, while $\tilde{\mathbf{q}}(x,y,t) = (\tilde{u},\tilde{v},\tilde{p},\tilde{\mathbf{T}})$ represents small amplitude disturbances. Replacing Eq. (4) in the conservation equations and non-Newtonian tensors (Eqs. (1) – (3)), we obtain a system of linearized equations for the disturbances, as long as non-linear terms are ignored, due to the infinitesimal amplitude of the disturbances (Schilichting, 1979).

Thus, the modal disturbances to be introduced are of the form

$$\tilde{\mathbf{q}}(x,y,t) = \overline{\mathbf{q}}(y)e^{i(\alpha x - \omega t)}. \tag{5}$$

where $\mathbf{q}$ refers to the velocity, pressure and tensor components, $i = \sqrt{-1}$ and $\overline{\mathbf{q}}(y)$ represents the amplitude of the disturbances. These equations indicate that disturbances propagate as waves with frequency ω, wavelength $\lambda = 2\pi/\alpha$ and wave speed $c = \omega/\alpha$, where α is the wavenumber in the x direction.

Thus, using the method of separating variables by normal modes, the system composed of conservation equations and non-Newtonian tensor equations is reduced to a system of differential equations

$$i\alpha\overline{u} + \frac{d\overline{v}}{dy} = 0, \tag{6}$$

$$\left(-i\omega + \frac{\partial U}{\partial x}\right)\overline{u} + V\frac{d\overline{u}}{dy} - \frac{\beta_{nn}}{Re_L}\frac{d^2\overline{u}}{dy^2} + \frac{\partial U}{\partial y}\overline{v} - \frac{d\overline{T}^{xy}}{dy} = \left(-\alpha i U - \frac{\beta_{nn}}{Re_L}\alpha^2\right)\overline{u} - \alpha i p + \alpha i\overline{T}^{xx}, \tag{7}$$

$$\frac{\partial V}{\partial x}\overline{u} + \left(-i\omega + \frac{\partial V}{\partial y}\right)\overline{v} + V\frac{d\overline{v}}{dy} - \frac{\beta_{nn}}{Re_L}\frac{d^2\overline{v}}{dy^2} + \frac{d\overline{p}}{dy} - \frac{d\overline{T}^{yy}}{dy} = \left(-\alpha i U - \frac{\beta_{nn}}{Re_L}\alpha^2\right)\overline{v} + \alpha i\overline{T}^{xy}, \tag{8}$$

$$Wi\frac{\partial \hat{T}^{xx}}{x}\overline{u} - 2Wi\hat{T}^{xy}\frac{d\overline{u}}{dy} + Wi\frac{\partial \hat{T}^{xx}}{\partial y}\overline{v} + \left(1 + Wi\left(-i\omega + 2\frac{\partial U}{\partial x}\right) + \alpha_G\frac{WiRe_L}{1-\beta_{nn}}2\hat{T}^{xx}\right)\overline{T}^{xx} + WiV\frac{d\overline{T}^{xx}}{dy} +$$
$$+ \left(-2Wi\frac{\partial U}{\partial y} + \alpha_G\frac{WiRe_L}{1-\beta_{nn}}2\hat{T}^{xy}\right)\overline{T}^{xy} = \left(2Wi\alpha i\hat{T}^{xx} + 2\frac{1-\beta_{nn}}{Re_L}i\alpha\right)\overline{u} - WiUi\alpha\overline{T}^{xx}, \tag{9}$$

$$Wi\frac{\partial \hat{T}^{xy}}{x}\overline{u} - \left(Wi\hat{T}^{yy} + \frac{1-\beta_{nn}}{Re_L}\right)\frac{d\overline{u}}{dy} + Wi\frac{\partial \hat{T}^{xy}}{\partial y}\overline{v} + \left(-Wi\frac{\partial V}{\partial x} + \alpha_G\frac{WiRe_L}{1-\beta_{nn}}\hat{T}^{xy}\right)\overline{T}^{xx} +$$
$$+ \left(1 - Wi\omega i + \alpha_G\frac{WiRe_L}{1-\beta_{nn}}(\hat{T}^{xx} + \hat{T}^{yy})\right)\overline{T}^{xy} + WiV\frac{d\overline{T}^{xy}}{dy} + \left(-Wi\frac{\partial U}{\partial y} + \alpha_G\frac{WiRe_L}{1-\beta_{nn}}\hat{T}^{xy}\right)\overline{T}^{yy} =$$
$$= \left(Wi\alpha i\hat{T}^{xx} + \frac{1-\beta_{nn}}{Re_L}i\alpha\right)\overline{v} - WiUi\alpha\overline{T}^{xy}, \tag{10}$$

$$Wi\frac{\partial \hat{T}^{yy}}{x}\overline{u} - 2\left(Wi\hat{T}^{yy} + \frac{1-\beta_{nn}}{Re_L}\right)\frac{d\overline{v}}{dy} + Wi\frac{\partial \hat{T}^{yy}}{\partial y}\overline{v} + \left(-2Wi\frac{\partial V}{\partial x} + \alpha_G\frac{WiRe_L}{1-\beta_{nn}}2\hat{T}^{xy}\right)\overline{T}^{xy} +$$
$$+ \left(1 + Wi\left(-i\omega - 2\frac{\partial V}{\partial y}\right) + \alpha_G\frac{WiRe_L}{1-\beta_{nn}}2\hat{T}^{yy}\right)\overline{T}^{yy} = \left(2Wi\alpha i\hat{T}^{xy}\right)\overline{v} - WiUi\alpha\overline{T}^{yy}. \tag{11}$$

In particular, for two-dimensional disturbances, if α is a real number ($\alpha_i = 0$ and $\alpha = \alpha_r$) and ω is a complex number, then the amplitude of the disturbance is increasing by the function of time. The components α_r, ω_r and ω_i represent, respectively, the wave number, frequency, and temporal growth rate, and this case consists of a temporal analysis of instabilities.

Now, if ω is a real number and α is a complex number, we have the amplitude of the disturbance increasing in the direction of the mean flow x. In this case, the answer will be a spatial analysis of the instabilities, and α_i is the spatial growth rate. In this work, in particular, the focus is on carrying out a spatial stability analysis in the boundary layer, and the classification of instabilities, based on temporal and spatial analyses, is presented in Tab. 1.

Table 1. Instabilities classification.

Type of analysis	Amplification rate	Amplitude	Classification
Spatial analysis	$\alpha_i < 0$	increase	unstable
	$\alpha_i = 0$	constant	neutral
	$\alpha_i > 0$	decreases	stable
Temporal analysis	$\omega_i < 0$	decreases	stable
	$\omega_i = 0$	constant	neutral
	$\omega_i > 0$	increase	unstable

The process of linearizing the system of equations and introducing normal modes leads to a system of differential equations in terms of the disturbance variables, which can be written as a generalized complex eigenvalue problem, of the form

$$\mathcal{L}(\hat{\mathbf{q}})[\overline{u} \quad \alpha\overline{u} \quad \overline{v} \quad \alpha\overline{v} \quad \overline{p} \quad \overline{T}^{xx} \quad \overline{T}^{xy} \quad \overline{T}^{yy}]^\top = \alpha\mathcal{R}[\overline{u} \quad \alpha\overline{u} \quad \overline{v} \quad \alpha\overline{v} \quad \overline{p} \quad \overline{T}^{xx} \quad \overline{T}^{xy} \quad \overline{T}^{yy}]^\top, \tag{12}$$

where $\mathcal{L}$ and $\mathcal{R}$ are matrices constructed in such a way that Eq. (12) is equivalent to the system composed of Eqs. (6) – (11), and are subject to appropriate boundary conditions. In particular, we adopt the no-slip wall condition for velocities

$$\tilde{u} = \tilde{v} = 0 \quad \text{para} \quad y = 0 \quad \text{e} \quad y = +\infty. \tag{13}$$

Thus, the instability modes are obtained by solving an eigenvalue problem, for which the first and second derivatives with respect to y $\left(\frac{d}{dy}, \frac{d^2}{dy^2}\right)$ are applied via differentiation matrices ($\mathcal{D}y, \mathcal{D}^2y$) calculated based on the Chebyshev spectral method. The solution that follows from Eq. (12) is called spatial modes.

4. BASEFLOW

In the present article, we adopt a base flow that consists of a flat plate boundary layer with zero angle of incidence, as we can see in Fig. 1. A spatial numerical simulation code, implemented based on the vorticity-velocity formulation, was

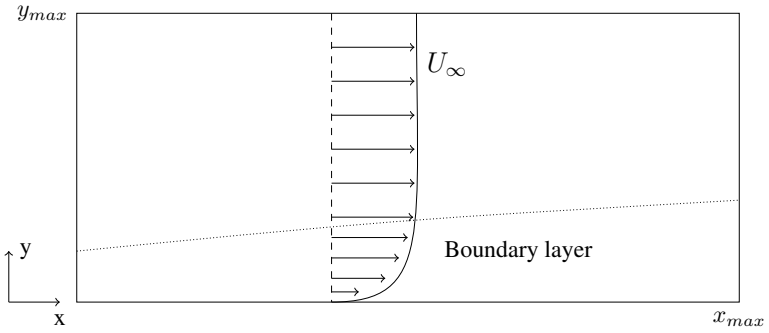

Figure 1. Computational domain for the flat plate boundary layer.

used to obtain this flow. The initial condition for the velocities and vorticity is defined by the Blasius similarity solution (Schilichting, 1979). The components of the non-Newtonian tensors are initialized as zero and the flow evolves until it reaches a steady state.

In particular, the choice for the vorticity-velocity formulation occurs due to the lack of need to deal with the pressure component and, therefore, simplifying the problem. Then, the two-dimensional vorticity ω_z is defined by

$$\omega_z = \frac{\partial u}{\partial y} - \frac{\partial v}{\partial x}. \tag{14}$$

Based on this formulation, the simulation consists of solving the system composed of Eqs. (15) – (20),

$$\frac{\partial U}{\partial x} + \frac{\partial V}{\partial y} = 0, \tag{15}$$

$$\frac{\partial^2 V}{\partial x^2} + \frac{\partial^2 V}{\partial y^2} = -\frac{\partial \hat{\omega}_z}{\partial x}, \tag{16}$$

$$\frac{\partial \hat{\omega}_z}{\partial t} + \frac{\partial \hat{\omega}_z}{\partial x}U + \frac{\partial \hat{\omega}_z}{\partial y}V = \frac{\beta_{nn}}{Re_L}\left[\frac{\partial^2 \hat{\omega}_z}{\partial x^2} + \frac{\partial^2 \hat{\omega}_z}{\partial y^2}\right] - \frac{\partial^2 \hat{T}^{xy}}{\partial x^2} - \frac{\partial^2 \hat{T}^{yy}}{\partial x \partial y} + \frac{\partial^2 \hat{T}^{xx}}{\partial y \partial x} + \frac{\partial^2 \hat{T}^{xy}}{\partial y^2}, \tag{17}$$

$$\hat{T}^{xx} + Wi\left(\frac{\partial \hat{T}^{xx}}{\partial t} + U\frac{\partial \hat{T}^{xx}}{\partial x} + V\frac{\partial \hat{T}^{xx}}{\partial y} - 2\hat{T}^{xx}\frac{\partial U}{\partial x} - 2\hat{T}^{xy}\frac{\partial U}{\partial y}\right) + \alpha_G \frac{WiRe_L}{1-\beta_{nn}}\left(\hat{T}^{xx^2} + \hat{T}^{xy^2}\right) = \\ = 2\frac{1-\beta_{nn}}{Re_L}\frac{\partial U}{\partial x}, \tag{18}$$

$$\hat{T}^{xy} + Wi\left(\frac{\partial \hat{T}^{xy}}{\partial t} + U\frac{\partial \hat{T}^{xy}}{\partial x} + V\frac{\partial \hat{T}^{xy}}{\partial y} - \hat{T}^{xx}\frac{\partial V}{\partial x} - \hat{T}^{yy}\frac{\partial U}{\partial y}\right) + \alpha_G \frac{WiRe_L}{1-\beta_{nn}}\left(\hat{T}^{xy}\left(\hat{T}^{xx} + \hat{T}^{yy}\right)\right) = \\ = \frac{1-\beta_{nn}}{Re_L}\left(\frac{\partial V}{\partial x} + \frac{\partial U}{\partial y}\right), \tag{19}$$

$$\hat{T}^{yy} + Wi\left(\frac{\partial \hat{T}^{yy}}{\partial t} + U\frac{\partial \hat{T}^{yy}}{\partial x} + V\frac{\partial \hat{T}^{yy}}{\partial y} - 2\hat{T}^{xy}\frac{\partial V}{\partial x} - 2\hat{T}^{yy}\frac{\partial V}{\partial y}\right) + \alpha_G \frac{WiRe_L}{1-\beta_{nn}}\left(\hat{T}^{xy^2} + \hat{T}^{yy^2}\right) = \\ = 2\frac{1-\beta_{nn}}{Re_L}\frac{\partial V}{\partial y}, \tag{20}$$

where Eq. (15) is the continuity equation, Eq. (16) is the Poisson equation for the V velocity component, obtained deriving Eq. (14) with respect to x. Equation (17) is obtained by deriving the momentum equation in direction y with respect to x and subtracting the derivative of the momentum equation in direction x with respect to y. Finally, Eqs. (18) – (20) are the Giesekus model equations for the non-Newtonian tensor in two-dimensional cartesian coordinates.

The temporal integration of the equations that describe the flow and the components of the extra-stress tensor in the context of viscoelastic flow is performed by a classical fourth-order Runge-Kutta scheme. Specifically, aiming to optimize

the numerical resolution in the region close to the rigid boundary in the y direction, we implemented a mesh stretching strategy. Furthermore, to deal with spatial derivatives, high-order compact finite difference schemes are applied, which require the solution of tridiagonal linear systems. We also incorporate methods to filter high-frequency oscillations in the flow direction. To solve the Poisson equation, we employ the FAS (Full Approximation Storage) scheme together with a Line Successive Overrelaxation (LSOR) method.

5. NUMERICAL RESULTS

The following results regarding the analysis of the stability of viscoelastic flows in a boundary layer on a flat plate were obtained through the Linear Stability Theory, with the base flow being generated from a spatial numerical simulation using the Blasius solution as the initial condition. The simulation parameters were selected such that $U_\infty = 5.2667m/s$, $L = 0.1m$ and $\nu = 1.59 \times 10^{-5}m^2/s$, resulting in a Reynolds number $Re_L = 33124$.

The domain of numerical integration in the flow direction extends from $x_0 = 1.0$ to $x_{max} = 16.8$ and goes from $y_0 = 0$ to $y_{max} = 0.36$ in the direction normal to the wall. The following parameters were adopted for the numerical simulation: the number of points in the streamwise and normal directions is $imax = 633$ and $jmax = 225$, respectively, being the distance between two consecutive points in the direction x, $\Delta x = 0.025$. The discretization in the y direction was performed using a mesh with a stretch factor of 10%.

Figure 2 illustrates the evolution of the velocity profile U along the flow, presenting velocity profiles at several fixed positions in the x direction for non-Newtonian flows. This specific case considers $Wi = 5$ and $\alpha_G = 0.2$ for $\beta_{nn} = 0.90, 0.80$ and 0.70. As the flow develops, it is possible to observe the influence of the fluid's viscoelasticity on the behavior
of the velocity U. Each spatial position in the domain in x corresponds to a value of Re, such that $Re = \sqrt{Re_L}\sqrt{x}$.

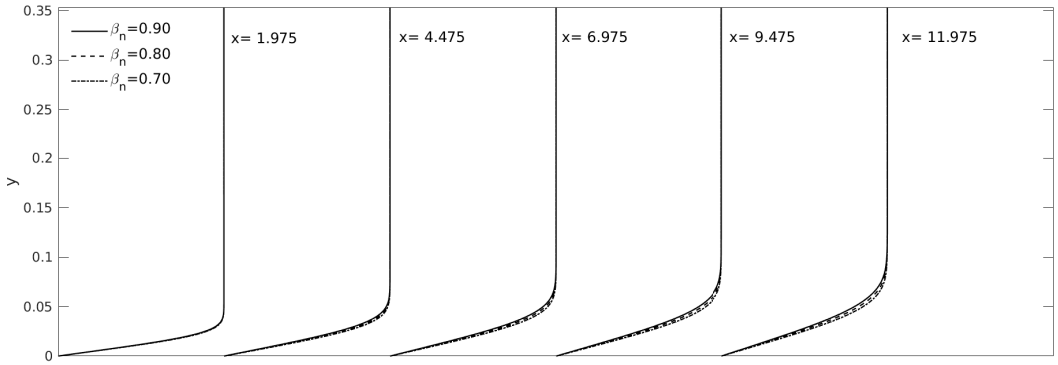

Figure 2. Evolution of streamwise velocity profiles U considering $Wi = 5$ and different values of β_{nn}.

To verify the influence of dimensionless parameters on flow stability, a variation of these parameters that characterize the viscoelastic fluid is carried out. Initially, the parameter α_G was set at 0.20 and then $\beta_{nn} = 0.90, 0.80$ and 0.70 was varied for $Wi = 1, 2, 3, 4, 5$ and 6. The numerical simulations provide the values of the spatial growth rates (α_i) for each of the cases considered.

In the case of a spatial analysis, growth rates less than zero ($\alpha_i < 0$) indicate instability in the flow, while growth rates greater than zero ($\alpha_i > 0$) indicate stability. Furthermore, as ω is a real value, the frequency F can be defined as $F = (\omega/Re_L) \times Re$ and the value used in the simulations was $F = 4$.

Figure 3 shows the spatial growth rate of the disturbances as a function of the flow direction x. It can be seen that the range of unstable frequencies is greater for flows with higher values of Wi, respectively, and increases even more as we decrease the value of β_{nn}.

Furthermore, cases where β_{nn} is smaller, that is, those with greater non-Newtonian contributions, achieve the highest growth rates. This is confirmed by Fig. 4, which shows the maximum growth rates for each of the tested cases. It is noted that the highest growth rates occur in flows with greater viscoelastic contribution and higher values of Wi. Furthermore, the decrease in β_{nn} further intensifies the growth of maximum growth rates with the increase in the value of Wi, which can be observed by the greater slope of the lines.

Still using the Linear Stability Theory, numerical simulations were carried out to determine the spatial growth rates (α_i) for different values of ω and Re (corresponding to each position in the flow direction), aiming to find the neutral stability curve, where $\alpha_i = 0$. In this diagram, growth rates less than zero ($\alpha_i < 0$, unstable) are inside the curve, while growth rates greater than zero ($\alpha_i > 0$, stable) are outside the curve.

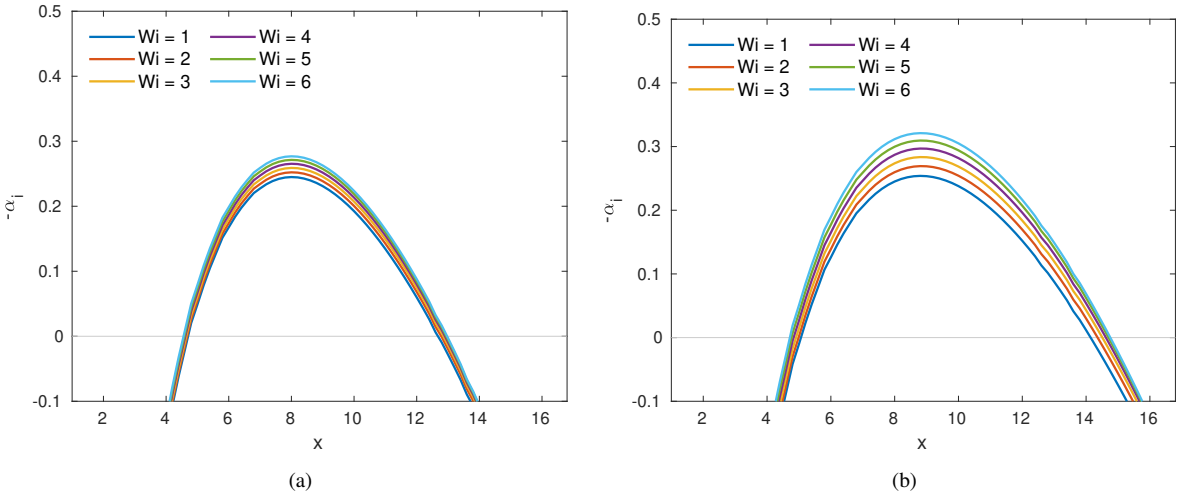

(a) (b)

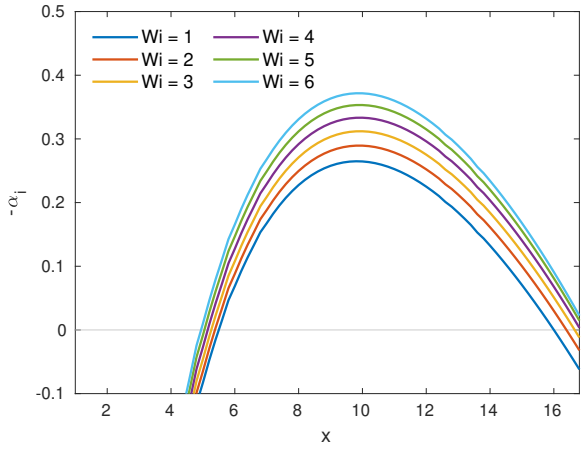

(c)

Figure 3. Spatial growth rate ($-\alpha_i$) as a function of streammwise direction for: (a) $\beta_{nn} = 0.90$; (b) $\beta_{nn} = 0.80$; and (c) $\beta_{nn} = 0.70$.

Figure 5 presents the neutral stability curves obtained by the LST analysis for viscoelastic flows, compared with the neutral curve in the Newtonian case. It is observed that in Fig. 5(a), the behavior of the curves for non-Newtonian cases is closer to the Newtonian case. On the other hand, Figs. 5(b) and 5(c), which represent the cases in which $\beta_{nn} = 0.80$

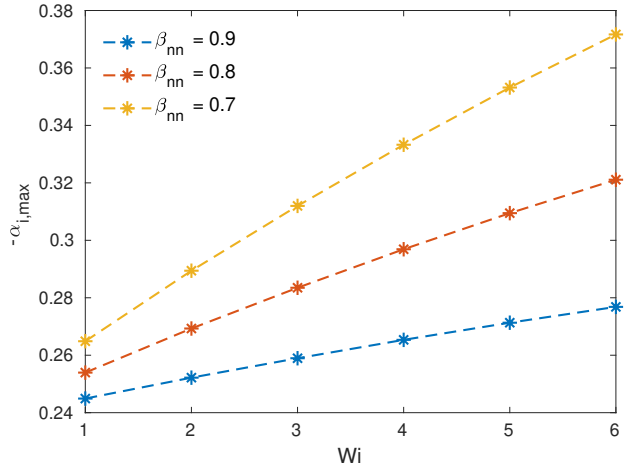

Figure 4. Maximun spatial growth rate ($-\alpha_i$).

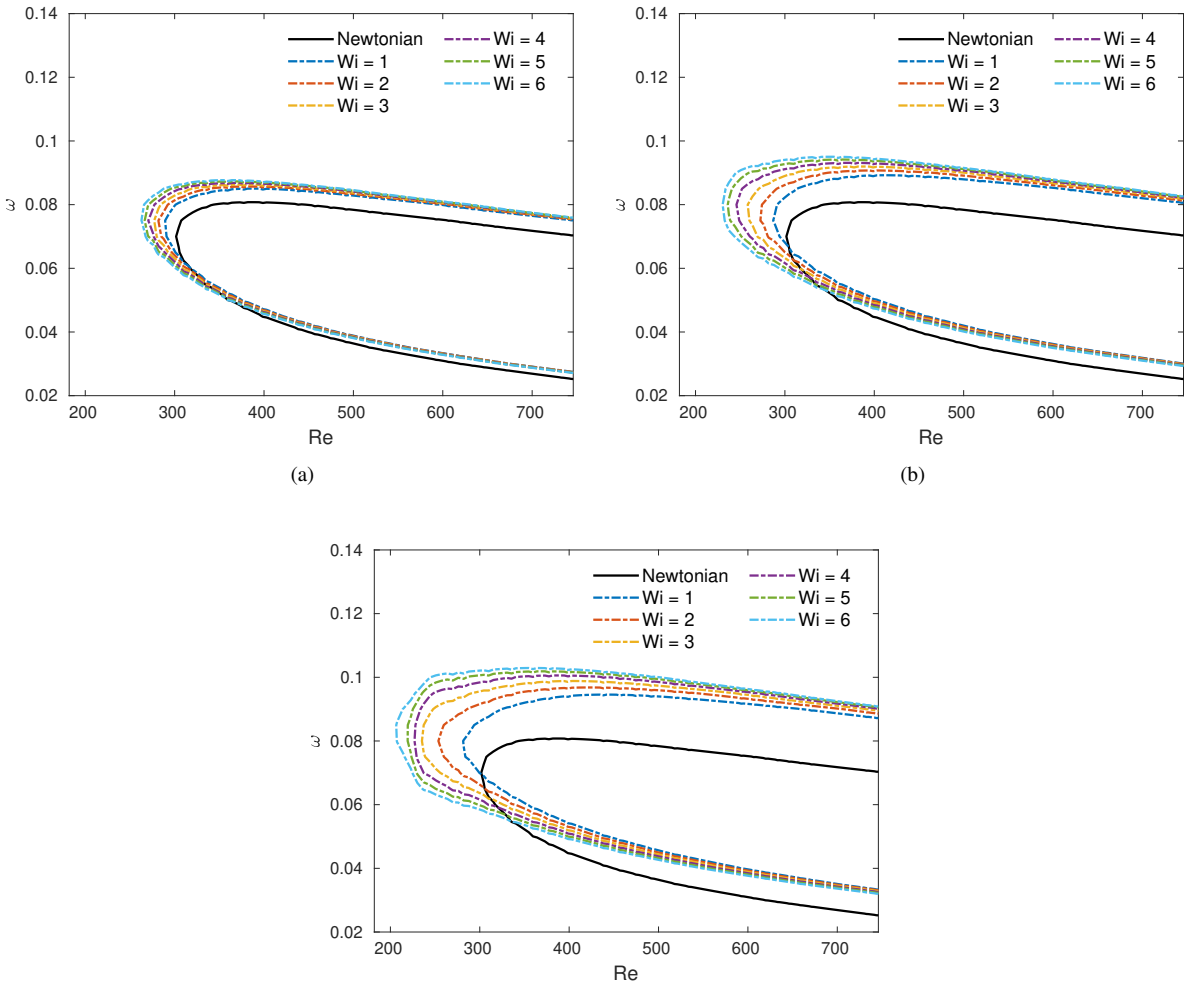

Figure 5. Stability diagrams considering Wi variations with: (a) $\beta_{nn} = 0.90$; (b) $\beta_{nn} = 0.80$; and (c) $\beta_{nn} = 0.70$.

and 0.70, show regions of greater instability. These regions increase as the value of Wi grows.

Furthermore, it is noted that the tip of the curve moves increasingly to the left as the value of Wi increases. The value of Re below which disturbances of any frequency are stable is called the critical Reynolds. Figure 6 confirms these observations, presenting the approximate values of critical Re. It is observed that this critical value increases with

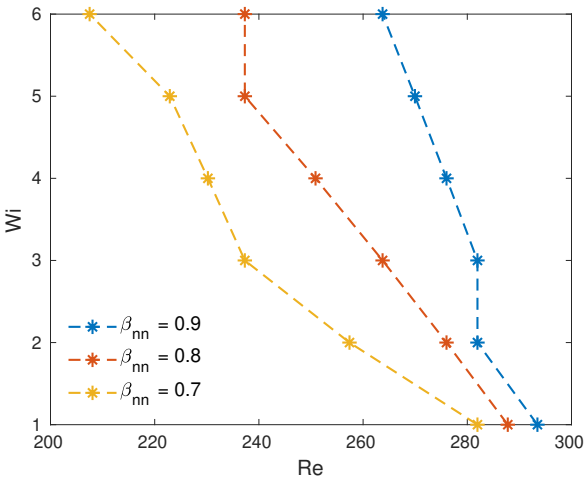

Figure 6. Approximate critical Reynolds values.

the increase of Wi and is even greater for the smallest values of β_{nn}. In other words, the greater the non-Newtonian contribution in the fluid, the lower the Reynolds value required for unstable regions to begin to emerge.

6. CONCLUSIONS

In this work, the Linear Stability Theory was used to investigate the hydrodynamic stability of a boundary layer flow over a flat plate, considering a viscoelastic fluid represented by the Giesekus model. The spatial growth rates of the disturbances were evaluated based on the results of several simulations, carried out by varying the dimensionless parameters characteristic of non-Newtonian fluid flow.

The results found allow us to verify that the variation of the constant β_{nn}, which is directly related to the non-Newtonian contribution in the fluid, interfered in the range of unstable frequencies of the flows, with flows with lower values of β_{nn} reaching the highest growth rates. The variation in the Weissenberg number (Wi) also significantly influenced flow stability, especially in fluids with a greater polymeric contribution.

The destabilizing effect of viscoelastic parameters was also confirmed by the results obtained for the neutral stability curves. It can be seen that flows with greater non-Newtonian contributions and higher values of Wi have larger unstable regions, which begin to emerge for much lower Reynolds values compared to the Newtonian case.

7. ACKNOWLEDGEMENTS

The authors acknowledge the National Council for Scientific and Technological Development (CNPq) or the research grant received during the development of this study. The research was carried out using the computational resource of the Center for Mathematical Applied to Industry (CeMEAI), funded by FAPESP (Process Number 2013/07375-0).

8. REFERENCES

Amoo, L.M. and Fagbenle, R.L., 2020. "Overview of non-newtonian boundary layer flows and heat transfer". In *Applications of Heat, Mass and Fluid Boundary Layers*, Woodhead Publishing, Woodhead Publishing Series in Energy, pp. 413–435.

Brandi, A.C., Mendonça, M.T. and Souza, L.F., 2019. "DNS and LST stability analysis of Oldroyd-B fluid in a flow between two parallel plates". *Journal Non-Newtonian Fluid Mechanics*, Vol. 267, pp. 14–27.

Cracco, M., 2019. *Linear Stability and Transient Behaviour of Viscoelastic Fluids in Boundary Layers.* Ph.D. thesis, Cradiff University, UK.

Gennaro, E.M., 2012. *Análise da estabilidade global de escoamentos compressíveis.* Ph.D. thesis, Universidade de São Paulo, São Carlos, SP.

Giesekus, H., 1982. "A simple constitutive equation for polymer fluids based on the concept of deformation-dependent tensorial mobility". *Journal of Non-Newtonian Fluid Mechanics*, Vol. 11, pp. 69–109.

Schilichting, H., 1979. *Boundary-Layer Theory*. McGraw-Hill, IncH.

Schubauer, G.B. and Skramstad, H.K., 1948. "Laminar boundary-layer oscillations and transition on a flat plate". *National Advisory Committee for Aeronautics*, Vol. TR-909.

Souza, L.F., Mendonça, M.T., Medeiros, M.A.F. and Kloker, M., 2002. "Analysis of Tollmien-Schilichting waves propagation on a flat plate with a Navier-Stokes solver". In *Proceedings of the 9th Brazilian Congress of Thermal Sciences and Engineering - ENCIT2002*.

Xu, H., Sherwin, S.J., Hall, P. and Wu, X., 2016. "The behaviour of Tollmien-Schlichting waves undergoing small-scale localised distortions". *Journal of Fluid Mechanics*, Vol. 792, p. 499–525.

Zhang, M., Lashgari, I., Zaki, T.A. and Brandt, L., 2013. "Linear stability analysis of channel flow of viscoelastic Oldroyd-B and FENE-P fluids". *Journal of Fluid Mechanics*, Vol. 737, pp. 249–279.

9. RESPONSIBILITY NOTICE

The authors are the only responsible for the printed material included in this paper.